Journal of Applied Polymer Science

Polymerization Shrinkage Evaluation on Nanoscale-Layered Silicates: Bis-GMA/TEGMA Nanocomposites, in Photo-Activated Polymeric Matrices

Luiza Mello de Paiva Campos,[1] Ademar Benévolo Lugão,[1] Mário Ramalho Vasconcelos,[2] Duclerc Fernandes Parra[1]

[1]Center of Chemistry and Environment, Institute of Nuclear and Energy Research, University of São Paulo, São Paulo, Brazil
[2]Department of Dental Materials, School of Dental Medicine, University of Porto, Porto, Portugal
Correspondence to: L.M.P. Campos (luizamello@usp.br)

ABSTRACT: This study concerns to the investigation of the polymerization shrinkage in dental experimental composites filled with silanized silica Aerosil® OX-50 and clay nanoparticulated Montmorilonita (MMT) Cloisite® 30B, in glycidyl methacrylate resin. The characterization of the experimental composites was established with the following analyses: Thermo-Mechanical Analysis (TMA) at isotherm temperature, Differential Scanning Calorimetry Analysis (DSC) under nitrogen atmosphere, X-Ray diffraction (DRX), and Micro Hardness analysis. Through the TMA analysis was observed that the polymerization shrinkage varies according to the filler type and concentration in the experimental composite. The polymerization shrinkage ranged from 0.98% to 0.22% in the experimental composites added with Cloisite® 30B and ranged from 2.73% to 1.01% in the experimental composites containing silanized silica. Due to the intercalation of the clay nanoparticle in relation to the polymer matrix, the experimental nanocomposites with Cloisite® 30B showed better performance compared to the composites with silanized silica. © 2013 Wiley Periodicals, Inc. J. Appl. Polym. Sci. **2014**, *131*, 40010.

KEYWORDS: polymerization shrinkage; biomaterials; resins; composites; nanostructured polymers; photo-polymerization

Received 20 March 2013; accepted 25 September 2013
DOI: 10.1002/app.40010

INTRODUCTION

Polymerization shrinkage is the main limitation in the use of dental composites. Some of the damage from the stresses caused by the polymerization process are: the emergence of gaps between the tooth and the restoration, detachment of the resin in relation to remaining tooth, cusps deflection, secondary caries, postoperative soreness and may even cause pulp changes, among others. The problem caused by the polymerization shrinkage is critical because the composite should be kept closely linked to tooth cavity while gaining stiffness and decreases its dimensions.[1,2]

The rupture of the interface between the dental restorative material and the dental substrate is caused by defective adhesive procedure or tensions involved in the interface tooth/ restoration. Among these, stresses generated during the polymerization of resin are described by many authors as the main cause of interfacial dislocation. [3–6]

The polymerization shrinkage presented by the resin matrix is a consequence of the establishment of covalent links between the monomers, decreasing the interatomic distance by 4–15 Å (relative to secondary interactions like Van der Walls). The polymerization of the Bis-GMA monomer occurs through the double bonds conversion of carbon of methacrylate groups. The resin systems contract primarily due to the formation of a polymer chain.[7,8] According to longitudinal clinical studies, the loss of marginal integrity is the main cause of restorations failure using composite resins.[9]

Gonçalvez et al.[10] reported that filler content increase reduced the unsaturation concentration and the polymerization stress, and decreased the volumetric shrinkage of the composite. The strong influence of the resin matrix on polymerization stress allowed the shrinkage reduction. Resin compositions at high level of filler, should have the compromise between low shrinkage and high conversion level.

One area of research that can be best explored is the polymers composites with mineral clays such as organic-modified Montmorillonite (MMT). These materials have attracted the interest of the plastic industry, due to improvements in mechanical, thermal, and optical properties.[11]

Some authors support the hypothesis that elastic forces developed during the polymerization in the galleries of clay are

responsible for lamellar intercalation and exfoliation. Lamellae adjacent to polymerization prevent folding due to electrostatic attractive forces between the quaternary ammonium ion and its negative counterpart, whereas Van der Walls forces between the organics fragments of quaternary ammonium ions work against exfoliation. In opposition, elastic forces from conformational entropy increase with growing molecular weight. Beyond a turning point, the elastics forces overcome the attractive forces and the adjacent layers move away from each other and lamellae distances are changed.[12,13] The organophilic clay addition in nanocomposites of polymeric matrix has the purpose of improving performance and life-span of dental composites, such as resistance to attrition, resistance to moisture absorption, control of polymerization shrinkage, mechanical, chemical, and physical properties of polymer matrices, other than reduction of costs and weight.[14,15]

Novel properties can be achieved as a result of surface interactions between the inorganic nanoparticulate and the polymeric matrix as the specific contact surface increases. As such, these materials appear compelling both for research and application. According to Fournaris et al.,[11] inorganic particles are incorporated into polymers as a means to maximize the Young modulus (elastic modulus) as well as lower the cost.

Some clay materials have the capacity to absorb organic molecules like MMT. This causes swelling as the lamellae are spread apart by polymerization occurring in between them. That kind of expansion may allow for a reduction of polymerization shrinkage as well as residual stress. Other authors have observed such a reduction in a Bis-GMA based system as clay mineral nanoparticles were added.[16,17] It is also possible that the increase in free volume inside the clay minerals contributed to that result.[13] Another study shows that the incorporation of clay nanoparticle Na-MMT in an adhesive photoactive matrix based around PMMA [poly(methyl methacrylate)] can result in the development of dental restoration composites with better physical, mechanical, and adhesion properties.[18]

The aim of this investigation was to evaluate and compare the influence of inorganic fraction on the polymeryzation shrinkage between the experimental nanocomposites added with Cloisite® 30B and experimental composites added with silanized silica Aerosil OX-50.

MATERIALS AND METHODS

The experimental composites were prepared manually by mixing the materials weighted and added to 1 g of the final composite mass.

The materials used to the experimental composites were: Bis-GMA [Bisphenol A Bis(2-hydroxy-3-methacryloxypropyl) Ether]. Lot: 688-51, Esstech, Essington, Pennsylvania; TEGDMA (Triethyleneglycol Dimethacrylate). Lot: PA02700018, Esstech, Essington, Pennsylvania. Camphorquinone, 97%. Lot: S12442-127, Sigma-Aldrich Chemie, GmbH, Steinheim, Germany. DMAEMA (2-(Dimethylamino)ethyl methacrylate), 98%. Lot: 21608009, Sigma-Aldrich Chemie, GmbH, Steinheim, Germany; Cloisite® 30B: MMT natural Cloisite® 30B. Lot: 09C02AAX015, Southern Clay Products, 1212 Church Street Gonzalez, Texas 78629; Silica: Aerosil® OX-50 Silanized. Lot: 091111. FGM, 89219-501, Joinville, SC, Brazil.

Cloisite® 30B

The clay mineral nanoparticle used in this study, MMT Cloisite® 30B, according to the manufacturer, was previously made organophilic through modification of its surface by methyl tallow bis-2-hidroxethyl (MT2EtOH) quaternary ammonium chlorine, with a concentration of 90 meq per 100 g of clay. Tallow refers to a mixture of alkyl compounds with approximately 65% in weight percent of C18, 30% of C16, and 5% of C14. MMT Cloisite® 30B possess $d_{001} = 18.5$ Å as the main X-ray diffraction peak, which also indicates its interlamellar spacing.

It is worth reminding that clay minerals are formed of tightly packed wide layers (which are called lamellae) with a height of around 1 nm and width ranging between 100 and 1000 nm.

Silanized Silica Aerosil® OX-50

The silica compound used in this study is constituted by particles with a radius of 0.04 μm or 40 nm. Its surface area, according to the manufacturer, is 48.3 m^2/g when not silanized and 26.2 m^2/g after it has been silanized.

Samples

The experimental composites groups were prepared with Cloisite® 30B and silanized silica Aerosil® OX-50 in six distinct formulations, varying according to the type and the concentration (in %) of inorganic filler, they were: Group 1—50% Cloisite® 30B; Group 2—60% Cloisite® 30B; Group 3—65% Cloisite® 30B; Group 4—50% Aerosil® OX-50; Group 5—60% Aerosil® OX-50; Group 6—65% Aerosil® OX-50.

The materials were weighed on an electronic digital precision scale, Shimadzu/model AY220. The experimental composites were manipulated by mixing the polymer and monomer. The Bis-GMA was incorporated into TEGDMA in a dappen pot in equal proportions (1 : 1) for all groups. In the sequence the camphorquinone and the tertiary amine DMAEMA were added. After 10 min of manual manipulation the inorganic filler was added in small amounts, continuously until the entire incorporation of that. For a correct homogenization of the mixture, the experimental composites were finally manipulated for 5 min Table I shows the formulation of the experimental composites used in this study.

The optimum thickness of samples was defined to be 0.50 mm. A Digital Caliper, Digital 6" model (0–150 mm) was used to check the samples' thicknesses.

The observed handling properties of the experimental compounds containing nanoparticles Cloisite® 30B and Aerosil silica OX-50 were similar to each, and the viscosity was close to that of commercial composites with high inorganic load content such as the compact resins used for posterior tooth preparation.

Thermo-Mechanical Analysis (TMA)

The TMA/SDTA840 measured dimensional changes of a sample in function of temperature using a quartz sensor. The test was established in isotherm program, at 25°C, operating simultaneously to the photo-polymerization LED Curing Light,

Table I. Formulation of the Experimental Composites

	Mass (g)					
	Group 1	Group 2	Group 3	Group 4	Group 5	Group 6
Bis-GMA	248	198	173	248	198	173
TEGDMA	248	198	173	248	198	173
Camphoroquinone	2	2	2	2	2	2
DMAEMA	2	2	2	2	2	2
Cloisite@ 30B	500	600	650	-	-	-
Aerosil OX-50@	-	-	-	500	600	650
Total mass	1000	1000	1000	1000	1000	1000

Kondorteck, model Aigh-7A, under photo-excitation of the sample at 468 nm wavelength, commonly used to the dental composite cure. The polymerization was monitored for a total time of 5 min, in which the light activation started after equilibrium of 30 s. During the photo-polymerization (3 min), the TMA recorded the main volumetric changes of the samples. Ten samples were tested for each group (1, 2, 3, 4, 5, and 6) and the results were obtained by the average percentage of polymerization shrinkage of three samples of each group, the standard deviation and variance was calculated.

This methodology measured the polymerization shrinkage in real time, during the cure process with a precision of 0.1 μm, to making it a simple, accurate and reliable measurement.

Scanning Differential Calorimetry (DSC)

The monitoring of cure and post-cure of composites were performed through calorimetry. The thermal enthalpy event attributed to the post-cure of the composites was investigated, after the polymerization, by DSC 822 Mettler–Toledo operating with samples of 20 mg in aluminum pan, heating program from 25 to 300°C, in dynamic atmosphere of N_2 at 50 mL min^{-1} and heating rate of 10°C min^{-1}, under a dynamic atmosphere of nitrogen. All DSC experiments were done in duplicate. The absence of exothermic event in DSC means the cure of the experimental composites.

X-ray Diffraction (DRX)

XRD diffractograms were obtained using a PAN analytical brand, model X'Pert PRO with X'Celerator detector, Rigaku D with Cu $K\alpha$ radiation ($\lambda = 1.54186$ Å, 45 kV, 40 A) at room temperature, the diffraction were scanned from 1.17° to 40° in 2θ range with 0.03° step at step/time 100 s. The analyses were conducted by the method of powder. The interlayer spacing was calculated according to Bragg's[19] [eq. (1)]:

$$n\lambda = 2d_{hkl} \sin \ominus \quad (1)$$

In which n is an integer, λ is the incident wavelength, d is the spacing between the planes of same $\{hkl\}$ (Miller index) in the crystal lattice, and θ is the angle between the incident ray and the crystal plane.

Micro-hardness

Micro-hardness analysis were performed on a Shimadzu, model HMV 200. The applied load was set 25 g for 10 s and the area analyzed was limited to the length of the longest diagonal of the Knoop indenter marks left on samples tested. Three samples were selected of each group for analysis and in each sample were done five indentations. The average was obtained from 15 samples in each group.

RESULTS

TMA

The results in percentage of the polymeryzation shrinkage, the variance, and the standard deviation are presented in Table II.

Figure 1 shows the performance comparison between the experimental nanocomposite with Cloisite® 30B and silanized silica Aerosil® OX-50 and different behavior was observed.

The result of the groups added with the silanized silica have linear behavior with $R^2 = 0.997$, which showed that the groups of experimental composites with higher amount of inorganic filler (65%), had a lower polymerization shrinkage.

However, the result of groups added with Cloisite® 30B, show nonlinear correlation ($R^2 = 0.915$), which reveals an interaction between the nanoparticles of clay and the polymer matrix.

DSC

Through DSC methodology was confirmed, the effectiveness of polymerization and conversion of the samples submitted to TMA methodology, comparing samples cured and uncured the same group.

DSC results showed that uncured and cured samples of the same group are distinct. Exothermic curves are reported by the heating DSC program showed of uncured samples, showing the

Table II. Results of the Polymerization Shrinkage

Group (type of sample)	Polymerization shrinkage (%)	Variance	Standard deviation
1 (50% Cloisite 30B)	0.98	0.16	0.40
2 (60% Cloisite 30B)	0.62	0.12	0.35
3 (65% Cloisite 30B)	0.22	0.05	0.00
4 (50% Silica)	2.73	0.26	0.69
5 (60% Silica)	1.51	0.03	0.18
6 (65% Silica)	1.01	0.12	0.34

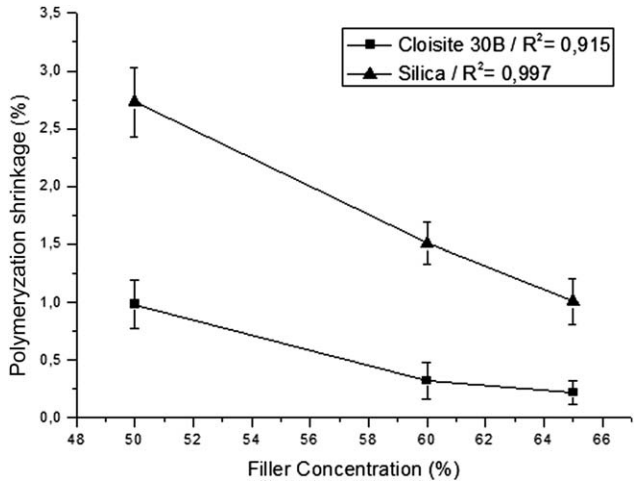

Figure 1. Performance comparison between the experimental nanocomposite added with Cloisite® 30B and the experimental composite added with silanized silica Aerosil® OX-50.

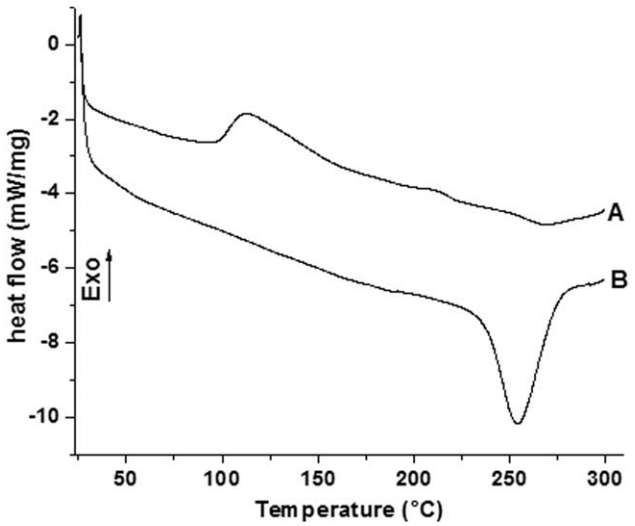

Figure 2. Cure curve comparison by DSC analysis of Group 1. (A) Uncured sample. (B) sample previously cured byTMA analysis.

polymerization stimulated by temperature, while in the samples previously polymerized, no post-cure event were observed. Therefore, the conditions used in the photo-polymerization technique associated to TMA shrinkage evaluation, allowed effective polymerization of the samples, and no exothermic reaction was caused by thermal effect as post-cure.

DSC of Group 1 is represented in Figure 2, where the uncured sample, top line on the graph, showed an exothermic phenomenon at around 110°C. The sample previously polymerized by TMA, represented by the bottom line, reported only the degradation event that began at about the 250°C, attributed to the polymer decomposition of the sample. All samples were subjected to DSC to confirm the effective photo-polymerization simultaneously to the TMA shrinkage evaluation and there were no post-curing event for any case.

DRX

The degree of exfoliation and dispersion of silicate layers of organomodified montmorillonite in the composites was investigated by XRD techniques from the position, shape, and the intensity of the basal reflections in the XRD patterns. Figure 3 reports the XRD patterns of organomodified MMT and their composites: "d" is the interplanar distance for the set of planes {hkl} (Miller index) of the crystal structure and $\ominus$ the angle of incidence of X-ray (measured between the incident beam and the crystal planes).

Figure 3(A,B) shows the XRD patterns of Cloisite® 30B pure and the XRD patterns of Groups 1, 2, and 3, respectively.

The original nanoclay Cloisite® 30B pure (A) peak "d_{001}" corresponded to 4.43 Å. Experimental composites filled with Cloisite® 30B (B) showed a displacement of the basal interplanar distance. The result obtained for interlayer spacing "d" presented by Group 1 was 2.51Å, Group 2: 2.59 Å, and Group 3: 2.56 Å, respectively.

This displacement in nanoclay indicates the occurrence of both intercalation and exfoliation phenomenon in the polymeric matrix based on Bis-GMA. Through evaluation of "d_{001}" value, directly related to the original spacing of the pure clay, compared to "d" values of Groups 1, 2, and 3, the dispersion's state of the clay in relation to the polymer matrix was determined. The displacement of the original "d_{001}" peak for smaller angles, or an increase in the interlayer space characterized the entry of the polymer into the clay layers.

Micro-hardness

The micro-hardness values of the experimental composites added with silanized silica Aerosil® OX-50 ranged from 11 to 15.

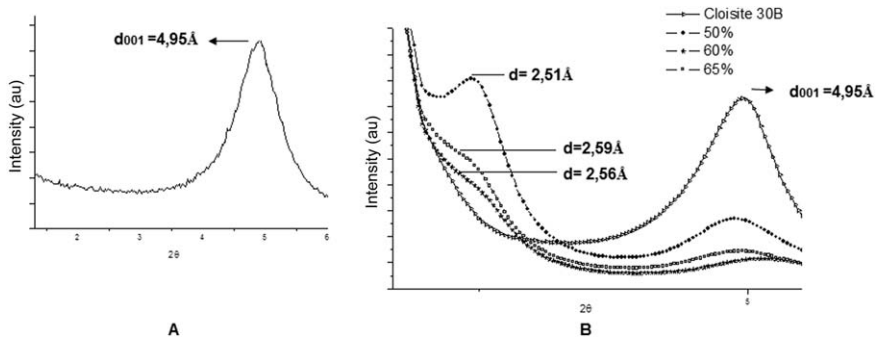

Figure 3. DRX diffratograms of nanoclay Cloisite® 30B (A) and nanocomposite of Groups 1, 2 and 3 (B).

These experimental composites followed the pattern of additive behavior of composites: with increasing the filler content, increased the micro-hardness value. However, the micro-hardness values of experimental nanocomposites added with Cloisite® 30B ranged from 18 to 22, showing higher values than the experimental composites added with silanized silica Aerosil® OX-50. The results of hardness for each group were: Group 1 = 18, Group 2 = 20, Group 3 = 22, Group 4 = 11, Group 5 = 13, and Group 6 = 15.

DISCUSSION

C=C bonds are scissed by the incidental radiation, which transfer energy on the weakest bonds of molecules. Consequently, new radicals are involved in the polymerization chain. The photo-irradiation generates intermediates for the propagation of curing. The Thermal Mechanical Analysis demonstrates the disappearance of unsaturation by the decrease in value of shrinkage polymerization (Table II), after the network bonds formation no shrinkage are observed.

Regarding to the TMA, Sakaguchi et al.[20] described in a critical paper, the evaluation of polymerization shrinkage by four methods, including the TMA. The authors have affirmed that the TMA methods have smaller sample volumes compared between the other techniques and the results was less affected by deformation along the surface (shrinkage), the Poisson effect and the compensation for deformation at the edges. In fact the 3 : 1 ratio between the diameters of the sample and the sensor of TMA used in this study, promoted the annulment of these effects. The authors in this study did not use any technique to verify the effects of post-cure. However, the results of this study showed no post-curing effect and the TMA method provided the maximum conversion, detectable by mechanical testing.

According to the results in all groups of experimental composites, the shrinkage polymerization was reduced as the inorganic filled increased, as expected, considering the minor polymeric matrix concentration. Regarding the performance of experimental composites in presence of silica Aerosil® OX-50, a typical profile shared by polymers containing inert particles was observed. A strong correlation between inorganic filled increase and the reduction in shrinkage polymerization was observed as the shrinkage decreased linearly ($R^2 = 0.997$). In the case of composites containing Cloisite® 30B ($R^2 = 0.915$) nanoparticles, a distinct profile was observed. Specifically, higher shrinkage polymerization levels were achieved at 50–60% filled concentrations and at 65% no relevant reduction was observed (Figure 1). The event seems to be related to the large amount of particles dispersed in the matrix. According to Solhi et Al.[18], after reached the optimum maximum level, the nanoparticles loading led to an induced aggregation state of nanoclay particles and reduced nanoparticles dispersion in the polymeric matrix.

The inorganic filler types used in this study showed influence on polymerization shrinkage by the mechanical behavior of the experimental composites. This fact reflects the shrinkage dependence of the interaction between polymer matrix and filler.

When comparing groups in presence of Cloisite® 30B (groups 1–3) and Aerosil OX-50 (groups 4–6) higher shrinkage polymerization levels were observed for the latter group. In particular, group 4 the led to a 278% increase in shrinkage polymerization over the group 1, while at 60% concentration (groups 2 and 5), the increase was around 243% and at 65% (groups 3 and 6) 458%. The characteristic of reinforcement of the clay is also performed when added to the polymer due to the restrictions on the mobility of polymer chains.[15]

In respect to the silica, interfacial adhesion between the filler particles and polymeric matrix is promoted by the silane groups containing in the surface.[10–23]

On the other hand, the improvement of the nanocomposites properties such as tensile strength and flexion, compression, fracture, impact, and the Young's modulus, have been related to clay dispersion and interfacial interactions polymer/clay, but no exclusively. The nanocomposites are distinguished from the conventional composites not because the particles have nanometric dimensions, but their properties are determined by these dimensions. The clay just dispersed in a polymeric matrix will act as conventional filler, but if intercalated and exfoliated in the polymer matrix during processing can act as a nanocomposite, promoting better characteristics of reinforcement. The additional advantage is that improved properties are obtained with concentrations below 5% by mass.[13,17,24] Formulations with high clay content showed mechanical properties not appropriated for practical applications in dentistry, however showed lower polymerization shrinkage.

The interaction between polymer/clay in this study was observed by XRD method and indicated an increasing in the interlayer space, effect of polymer intercalation into the clay galleries. This interaction between polymer/clay justified the higher micro hardness values of the groups added with Cloisite® 30B in relation to those with silica Aerosil® OX-50. The chemical affinity between the Bis-GMA/TEGDMA based polymeric matrix and the Cloisite® 30B clay mineral nanoparticle (whose surface is rendered organophilic by the modification with methyl tallow bis-2-hidroxethyl (MT2EtOH; quaternary ammonium salt) may have had a determining role, not only in its better mechanical performance, but also in causing a reduction of polymerization shrinkage.

According to some authors, the ability of certain clays to absorb organic molecules, increase lamellae distances themselves from each other, developing an additional volume within the material. The authors' hypothesis was that expansive nature of the clay could reduce the magnitude of polymerization shrinkage and residual stress of the composites.[17–25]

Pertaining micro-hardness, the experimental composites filled with Cloisite® 30B reached higher values when compared to composites filled with Silica OX-50. This fact is attributed to the high hardness levels and the high modulus of the

nanoclay.[26] Nanometric particles hold higher contact surfaces with the matrix which may contribute to the increase in mechanical properties.[27]

CONCLUSION

The thermo-mechanical analysis proved to be effective in the characterization and measurement of polymerization shrinkage of experimental nanocomposites.

The analysis of XRD showed the intercalation phenomenon of the polymer matrix in relation to clay nanoparticles in the experimental nanocomposites added with Cloisite® 30B, explaining the lower values of polymerization shrinkage and the higher values of micro-hardness.

The groups of experimental composites filled with silanized silica Aerosil® OX-50, showed typical behavior of the composites with inert and additive filler. On the other hand, the groups with higher concentration of inorganic filler showed the lowest value of polymerization shrinkage and the highest values of micro-hardness. Due to the intercalation of the clay nanoparticle in relation to the polymer matrix, the experimental nanocomposites with Cloisite® 30B, showed better performance compared to the composites with silanized silica as well as lower polymerization shrinkage.

ACKNOWLEDGMENTS

The authors thank to ESSETECH, SOUTHERN CLAY PRODUCTS, and FGM for donating the materials; CNPQ and CAPES for funding this project; Technological Characterization Laboratory of Department of Mining and Petroleum, University of São Paulo (LCT-EPUSP) for DRX tests; Department of Dental Materials, School of Dentistry, University of São Paulo (FOUSP) for the Micro Hardness tests. FAPESP process no. 2012/00236/1.

REFERENCES

1. Kleverlaan, C.J.; Feilzer, A. J. *Dent. Mater.* **2005**, *21*, 1150.
2. Venhoven, B. A.; De Gee A. J.; Davidson, C. L. *Biomaterials* **1993**, *14*, 871.
3. Davidson, C. L.; Davidson-Kaban, S. S. *Dent. Update* **1998**, *25*, 274.
4. Ferracane, J. L. *Dent. Mater.* **2005**, *21*, 36.
5. Calheiros, F. C.; Sadek, F. T.; Braga, R. R.; Cardoso, P. E. *J. Dent.* **2004**, *32*, 407.
6. Braga, R. R.; Ferracane, J. L. *Crit. Rev. Oral Biol. Med.* **2004**, *15*, 176.
7. Peutzfeldt, A. *Eur. J. Oral Sci.* **1997**, *10*, 97.
8. Dewaele, M.; Truffier-Boutry, D.; Devaux, J.; Leloup, G. *Dent. Mater.* **2006**, *22*, 359.
9. Watts, D. C.; Cash, A. *J. Dent. Mater.* **1996**, *7*, 281.
10. Gonçalvez, F.; Azevedo, C. L. N.; Ferracane, J. L.; Braga, R. R. *Dent. Mater.* **2010**, *27*, 520.
11. Fournaris, K. G.; Boukos, N.; Petridis, D. *Appl. Clay Sci.* **2001**, *19*, 77.
12. Park, J. H.; Jana, S.C. *Macromolecules* **2003**, *36*, 2758.
13. Discacciati, J. A. C.; Oréfice, R. L. *Proc. Polym. Am. Reg. Meet.* **2004**, *1*, 42.
14. Ray, S. R.; Okamoto, M. *Prog. Polym. Sci.* **2003**, *28*, 1539.
15. Discacciati, J. A. C.; Oréfice, R. L. *J. Mater. Sci.* **2007**, *42*, 3883.
16. Kelly, P.; Akelah, A.; Qutubuddin, S.; Moet, A. *J. Mater. Sci.* **1994**, *29*, 2274.
17. Salahudin, N.; Shehata, M. *Polymer* **2001**, *42*, 8379.
18. Solhi, L.; Atai, M.; Nodehi, A.; Imani, M. *Dent. Mater.* **2012**, *28*, 1041.
19. Cullity, B. D. *Elements of X-Ray Diffraction*, 2nd ed.; Reading, Addinson-Wesley, **1978**; p 555.
20. Sakaguchi, R. L.; Wiltbank, B. D.; Shah, N. C. *Dent. Mater.* **2004**, *20*, 388.
21. Jones, D. W.; Rizkalla, A. S. *J. Biomed. Mater. Res.* **1996**, *33*, 89.
22. Masouras, K.; Silikas, N.; Watts, D. C. *Dent. Mater.* **2008**, *24*, 932.
23. Garoushi, S.; Vallittu, P. K.; Watts, D. C.; Lassila, L. V. *Dent. Mater.* **2008**, *24*, 606.
24. Liu, Y.; Tan, Y.; Lei, T.; Xiang, Q.; Han, Y.; Huang, B. *Dent. Mater.* **2009**, *25*, 709.
25. Harrats, C.; Groeninckx, G. *Macromol. Rapid. Commun.* **2008**, *29*, 14.
26. Hussain, F.; Chen, J.; Hojjati, M. *Mater. Sci. Eng. A* **2007**, 445–446, 467.
27. Wang, S. *Polym. Degrad. Stab.* **2002**, *77*, 423.